An algorithm for computing the deflection angle of surface ocean currents relative to the wind direction

Adrian Constantin[1], David G. Dritschel[2], and Nathan Paldor[3]

[1]University of Vienna
[2]Mathematical Institute, University of St Andrews, UK
[3]Hebrew University of Jerusalem

November 22, 2022

Abstract

The angle between the wind stress that overlies the ocean and the resulting current at the ocean surface is calculated for a two-layer ocean with uniform eddy viscosity in the lower layer and for several assumed eddy viscosity profiles in the upper layer. The calculation of the deflection angle is greatly simplified by transforming the linear, second order, vertical structure equation to its associated nonlinear, first order, Riccati equation. Though the transformation to a Riccati equation can be used as an alternate numerical scheme, its main advantage is that it yields analytic expressions for particular eddy viscosity profiles.

An algorithm for computing the deflection angle of surface ocean currents relative to the wind direction

Adrian Constantin[1], David G. Dritschel[2], Nathan Paldor[3]

[1]Department of Mathematics, University of Vienna,
Vienna 1090, Austria

[2]School of Mathematics and Statistics, University of St Andrews,
St Andrews KY16 9SS, UK

[3]The Fredy and Nadine Herrmann Institue of Earth Sciences, The Hebrew University of Jerusalem,
Jerusalem 9190401, Israel

June 26, 2020

Abstract

The angle between the wind stress that overlies the ocean and the resulting current at the ocean surface is calculated for a two-layer ocean with uniform eddy viscosity in the lower layer and for several assumed eddy viscosity profiles in the upper layer. The calculation of the deflection angle is greatly simplified by transforming the linear, second order, vertical structure equation to its associated nonlinear, first order, Riccati equation. Though the transformation to a Riccati equation can be used as an alternate numerical scheme, its main advantage is that it yields analytic expressions for particular eddy viscosity profiles.

1 Introduction

For wind-driven surface ocean currents, various ranges of the deflection angle are recorded (see *Röhrs and Christensen*, 2015). Predictions for the deflection angle are only available for special profiles of vertical eddy viscosities (see the discussions in *Bressan and Constantin*, 2019; *Constantin*, 2020; *Dritschel et al.*, 2020). Numerical approaches for depth-dependent eddy viscosities rely on the WKB approach (see *Wenegrat and McPhaden*, 2016) to find accurate approximations for the solution of the second-order boundary-value problem that governs Ekman flows. The WKB approximation consists of a rapidly oscillating complex exponential multiplied by a slowly varying amplitude, and requires that the properties of the medium vary more slowly than the solution (see the discussion in *Holmes*, 2013). In particular, the eddy viscosity should vary gradually with depth, an assumption that limits the applicability of the WKB approach.

In this paper we derive a uniformly valid formula for the deflection angle that, rather than relying on solving a second-oder boundary-value problem on an interval of infinite length, only requires the solution of a first-order initial-value problem, with a suitable Riccati equation, on a finite interval.

Note that the Riccati equation arises in many different fields of physics and engineering, e.g. control theory, statistical thermodynamics, quantum mechanics, cosmology (see the survey in *Schuh*, 2014). In light of this, its relevance to the study of wind-driven currents is perhaps not that surprising.

2 The proposed algorithm

The non-dimensional linear governing equations for steady wind-driven ocean currents in the non-equatorial Northern Hemisphere are (see *Dritschel et al.*, 2020)

$$(K\psi')' - 2\mathrm{i}\psi = 0 \quad \text{for} \quad z < 0\,, \tag{1}$$

$$\psi'(0) = 1 \qquad \text{on} \quad z = 0\,, \tag{2}$$

$$\psi \to 0 \qquad \text{as} \quad z \to -\infty\,, \tag{3}$$

where the complex vector $\psi = u + \mathrm{i}v$ represents the horizontal velocity field, z is the upward pointing vertical variable (with the free surface at $z = 0$) scaled on $\sqrt{(2\tau/\rho)}/f$ (where τ is the applied wind stress at the ocean's surface, ρ is the water density and f is the constant Coriolis parameter) and $K(z)$ is the vertical (depth-dependent) non-dimensional eddy viscosity (that equals the dimensional eddy viscosity scaled on τ/f). Since the turbulence is practically confined to a near-surface ocean layer, it is reasonable to assume that below a certain depth h the eddy viscosity is equal to the molecular viscosity of sea water, normalised so that

$$K(z) = 1 \quad \text{for} \quad z \leq -h\,, \tag{4}$$

with $K(z) > 0$ for $z \in (-h, 0]$ unconstrained, other than by a continuous dependence on z. The deflection angle from the wind direction at the surface is the argument of the complex vector $\psi(0)$. For $K \equiv 1$ the unique solution to (1)-(2)-(3) is

$$\psi(z) = \frac{1}{1+\mathrm{i}}\,\mathrm{e}^{(1+\mathrm{i})z}\,, \qquad z \leq 0\,,$$

with $\psi(0) = \frac{1}{\sqrt{2}}\,\mathrm{e}^{-\mathrm{i}\frac{\pi}{4}}$ corresponding to a deflection angle of $\frac{\pi}{4}$ (which we'll denote below as 45^o) to the right of the wind direction; this is the classical result of *Ekman* (1905).

Let us now present the algorithm that we propose for the calculation of the deflection angle for general continuous depth-dependent eddy viscosities, the justification of the procedure being provided in the next section.

1. Solve the Riccati equation

$$q'(z) + \frac{1}{K(z)}\,q^2(z) = 2\mathrm{i} \quad \text{on} \quad (-h, 0)\,, \tag{5}$$

   with "initial" data

$$q(-h) = 1 + \mathrm{i}\,. \tag{6}$$

2. With $q(0)$ computed in Step 1, the deflection angle is

$$\arg[\psi(0)] = -\arg[q(0)]\,. \tag{7}$$

Note that the Riccati equation is essentially the only ordinary differential equation admitting a nonlinear superposition principle, a remarkable feature ensuring the existence of a symmetry group and leading to integrability conditions (see *Cariñena and Ramos*, 1999). However, equation (5) is not, in general, solvable by quadratures (see the discussion in *Hille*, 1997) and in general one has to rely on numerical methods to obtain accurate approximations of the unique solution to the initial-value problem (5)-(6).

3 Methods

Let us now justify the algorithm described in Section 2.

Equation (1) simplifies on $(-\infty, -h)$ to

$$\psi'' = 2\mathrm{i}\psi\,, \qquad z < -h\,, \tag{8}$$

for which the general solution is a linear combination of the linearly-independent functions $\mathrm{e}^{\pm(1+\mathrm{i})z}$. If we denote by $\psi_\pm$ the solutions of (1) with

$$\psi_\pm(z) \propto \mathrm{e}^{\pm(1+\mathrm{i})z}\,, \qquad z < -h\,, \tag{9}$$

then we have a fundamental system of solutions for (1). The asymptotic behaviour (3) thus ensures that the solution ψ to (1) satisfies

$$\psi(z) = C\,\psi_+(z)\,, \qquad z \le 0\,, \tag{10}$$

for some complex constant C determined by the boundary condition (2). Differentiating (10) and evaluating the outcome and equation (10) at $z = 0$, we find

$$\psi(0)\,\psi_+'(0) = \psi_+(0)\,, \tag{11}$$

taking (2) into account. It is known (see *Constantin*, 2020) that $\psi(z) \neq 0$ for all $z \le 0$. Consequently (10) yields $\psi_+(z) \neq 0$ for all $z \le 0$ and $C \neq 0$, while from (10) and (11) we get

$$C = \frac{1}{\psi_+'(0)} = \frac{\psi(0)}{\psi_+(0)}\,. \tag{12}$$

Now consider the function

$$q(z) = \frac{K(z)\,\psi_+'(z)}{\psi_+(z)}\,, \qquad z \le 0\,. \tag{13}$$

From (1) we obtain

$$q'(z) + \frac{q^2(z)}{K(z)} = 2\mathrm{i}\,, \qquad z < 0\,,$$

with

$$q(z) = 1 + \mathrm{i}\,, \qquad z \le -h\,,$$

due to (9). Consequently the restriction of the function q to $[-h, 0]$ is the unique solution of the initial-value problem (5) and (6). On the other hand, (11)-(13) yield

$$q(0) = \frac{K(0)}{\psi(0)}\,. \tag{14}$$

Since $K(0)$ is real, relation (7) emerges. The proposed algorithm is therefore validated.

Remark. The proposed algorithm also yields the horizontal velocity field. Indeed, using (10), integrating (13) and taking (11) and (14) into account, we get

$$\psi(z) = \frac{K(0)}{q(0)} \exp\left\{ -\int_z^0 \frac{q(s)}{K(s)}\,\mathrm{d}s \right\}, \qquad z \in [-h, 0]\,. \tag{15}$$

On the other hand, (9), (10) and (12) yield

$$\psi(z) = \frac{\psi(-h)}{\psi_+(-h)}\,\mathrm{e}^{(1+\mathrm{i})z} = \psi(-h)\,\mathrm{e}^{(1+\mathrm{i})(z+h)}\,, \qquad z < -h\,,$$

and consequently

$$\psi(z) = \frac{K(0)}{q(0)} \exp\left\{ (1+\mathrm{i})(z+h) - \int_{-h}^0 \frac{q(s)}{K(s)}\,\mathrm{d}s \right\}, \qquad z < -h\,. \tag{16}$$

since $\psi(-h)$ can be computed from the formula (15). $\square$

4 Examples

We now present some examples of solutions to the initial-value problem (5) and (6). Since $K(z) = 1$ for $z \leq -h$, it suffices to specify a continuous function $K : [-h, 0] \to (0, \infty)$ with $K(-h) = 1$.

4.1 The quadratic profile

For the quadratic polynomial

$$K(z) = [a(z+h)+1]^2\,, \qquad z \in [-h, 0]\,,$$

the substitution $Q(z) = q(z)/(a(z+h)+1)$ transforms (5) and (6) to the equivalent initial-value problem

$$Q'(z) = \frac{2\mathrm{i} - aQ(z) - Q^2(z)}{a(z+h)+1}\,, \qquad z \in (-h, 0)\,, \tag{17}$$

$$Q(-h) = 1 + \mathrm{i}\,. \tag{18}$$

To ensure the regularity of $Q(z)$ the values of a and h have to satisfy $ah > -1$. The differential equation (17) is separable and can be straightforwardly integrated, yielding

$$\ln\left(\frac{Q(z) + \frac{a+\zeta}{2}}{Q(z) + \frac{a-\zeta}{2}}\right) = \ln\left(\frac{1 + \mathrm{i} + \frac{a+\zeta}{2}}{1 + \mathrm{i} + \frac{a-\zeta}{2}}\right) + \frac{1}{a\zeta}\,\ln[a(z+h)+1]\,, \qquad z \in [-h, 0]\,,$$

where

$$\zeta = \sqrt[4]{a^4 + 64}\,\exp\left[\frac{\mathrm{i}}{2}\,\arctan\left(\frac{8}{a^2}\right)\right].$$

Since $q(0) = (1 - ah)Q(0)$, an explicit formula for the deflection angle (7) emerges, dependent on the parameters a and h.

4.2 The $4/3$ power-law profile

For

$$K(z) = [3(z+h)+1]^{\frac{4}{3}}\,, \qquad z \in [-h, 0]\,,$$

the general solution of (5) is

$$q(z) = -S(z) - (1-\mathrm{i})S^2(z)\tan\Big((1-\mathrm{i})S(z) + C\Big)\,, \qquad z \in [-h, 0]\,,$$

where $S(z) = [3(z+h)+1]^{\frac{1}{3}}$, while C is a complex constant determined by the boundary condition (6). Using the complex identity $\arctan(z) = \frac{1}{2\mathrm{i}}\,\tan\left(\frac{\mathrm{i}-z}{\mathrm{i}+z}\right)$ we find

$$C = -1 + \mathrm{i} + \tfrac{\mathrm{i}}{2}\,\ln\left(\tfrac{1-\mathrm{i}}{\mathrm{i}-5}\right).$$

4.3 The linear profile

Madsen (1977) investigated an infinitely deep ocean with an eddy viscosity that increases linearly with depth from a value of zero at the free surface. For $\mu > 0$, the eddy viscosity profile

$$K(z) = \mu + \frac{\mu - 1}{h}\,z\,, \qquad z \in [-h, 0]\,,$$

equals μ at the surface and decreases/increases with depth, according to whether $\mu > 1$ or $\mu \in (0, 1)$, respectively. In this case the general solution of (5) is available in terms of the Bessel functions J_1 and Y_1 (see *Polyanin and Zaitsev*, 2013).

$$q(z) = \frac{2\mathrm{i}h}{\mu - 1} \frac{Q(x)}{Q'(x)} \quad \text{with} \quad Q(x) = \sqrt{x} \left[C_1 J_1 \left(\zeta \sqrt{x} \right) + C_2 Y_1 \left(\zeta, \sqrt{x} \right) \right]$$

where C_1 and C_2 are chosen such that their ratio satisfies the boundary condition (6), while $\zeta = 2h(1-\mathrm{i})/(|\mu - 1|)$ and $x = \mu + z(\mu - 1)/h$ ranges between 1 and μ. Note that (6) becomes:

$$1 + \zeta \left(\frac{C_1 J_1'(\zeta) + C_2 Y_1'(\zeta)}{C_1 J_1(\zeta) + C_2 Y_1(\zeta)} - 1 \right) = 0$$

which determines the ratio C_1/C_2 purely in terms of ζ; notably the solution $q(z)$ depends only on this ratio.

5 Results

In this section, we examine how the surface deflection angle θ_0 varies with the value of the surface eddy viscosity $K(0)$ and the depth h of the upper layer of variable eddy viscosity, for the three examples provided in the previous section. To gain further insight, we also compare the deflection angle obtained from the associated Riccati equation with the case of constant eddy viscosity in the upper layer that was examined previously in *Dritschel et al.* (2020).

The analytical expressions obtained for the three examples above were checked numerically by directly integrating the Ricatti equation (5) (a simple `Python` code, entitled ekman_sipral.py which may be adapted for any continuous $K(z)$ is available on zenodo: 10.5281/zenodo.3904295). In most cases the exact and numerical expressions for $q(z)$ agree within around 10^{-7} (similar to the tolerance of the ODE integrator used). Exceptions occur only when $K(0) \ll 1$, i.e. when (5) is nearly singular at $z = 0$. In the singular case $K(z) \sim -\gamma z$ as $z \to 0$ (here $\gamma > 0$), one can show that to leading order $q(z) \sim -\gamma / \ln(-z)$ as $z \to 0$ a dependence which is difficult to accurately capture by the ODE integrator without modifying the equation. As this is not an important case, no effort was made to do this.

We start with the 4/3 power law discussed in section 4.2 since this case depends only on a single parameter, h, and is therefore simplest. The surface deflection angle θ_0 is plotted as a function of h in figure 1 (note the log scaling of h). For $h \ll 1$, as expected $\theta_0 \approx 45°$ since in this case $K \approx 1$ throughout the shallow upper layer. The largest deflection occurs for $h \approx 2.463$, for which $\theta_0 \approx 62.22654°$. At larger depths, the surface deflection angle decreases again, slowly approaching 45° in the limit $h \to \infty$ (which also corresponds to infinite surface eddy viscosity). One can show that $\tan\theta_0 \approx 1 + (3h)^{-1/3}$ for $h \gg 1$.

Next we consider the upper-layer eddy viscosity $K(z) = [a(z + h) + 1]^2$ whose analytical solution is provided in section 4.1. This now depends on two parameters, a and h. To facilitate comparisons with other profiles of $K(z)$, we use the surface eddy viscosity $K(0) = (ah+1)^2 \equiv \mu$ as the control parameter instead of a, alongside the upper layer depth h. The dependence of the surface deflection angle θ_0 on μ and h is shown in figure 2 over an extensive range of parameter values. First of all, when $\mu = 1$, $K(z) = 1$ for all z and $\theta_0 = 45°$; this is the constant viscosity case examined originally by *Ekman* (1905). When $\mu > 1$, the deflection angle in increased, while when $\mu < 1$, it is decreased. The biggest change in θ_0 depends on h, favouring small h when $\mu \ll 1$ and large h when $\mu \gg 1$. In fact, the biggest change occurs roughly on the curve $h = 0.7\mu^{1/4}$, found by a least squares fit to $\log_{10} h = c_0 + c_1 \log_{10} \mu$. While the fit is not perfect, the variance in $\log_{10} h$ is only 0.0175 over the range of $\log_{10} \mu$ considered.

We next examine the linear upper-layer eddy viscosity profile $K(z) = (\mu - 1)(z + h)/h + 1$ introduced in section 4.3. The dependence of θ_0 on μ and h is shown in figure 3 over the

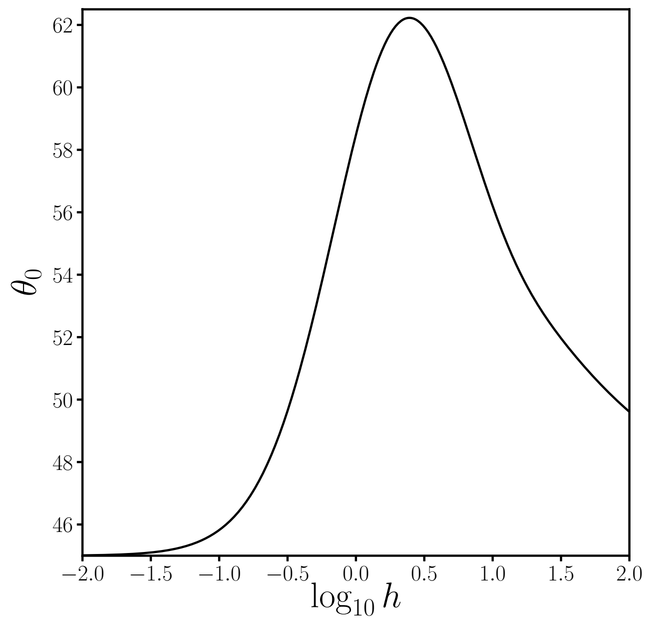

Figure 1: Surface deflection angle θ_0 (in degrees) as a function of the non-dimensional depth h of the upper layer when $K(z) = [3(z + h) + 1]^{\frac{4}{3}}$ there and $K(z) = 1$ below.

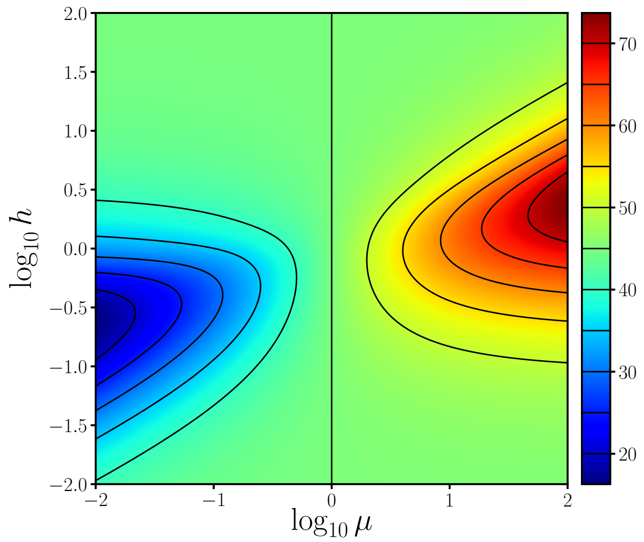

Figure 2: Surface deflection angle θ_0 (in degrees) as a function of the surface eddy viscosity μ and non-dimensional depth h of the upper layer when $K(z) = [(\sqrt{\mu} - 1)(z + h)/h + 1]^2$ there.

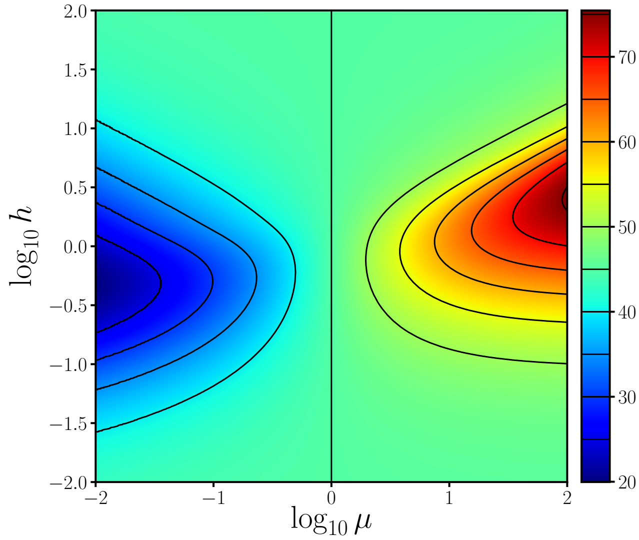

Figure 3: Surface deflection angle θ_0 (in degrees) as a function of the surface eddy viscosity μ and non-dimensional depth h of the upper layer when $K(z) = (\mu - 1)(z + h)/h + 1$ there.

same range of parameter values considered in figure 2. The results are broadly similar, with a decrease in θ_0 from $45°$ for $\mu < 1$ and an increase for $\mu > 1$. For $\mu > 1$, the results compare surprisingly closely, but this is not true for $\mu < 1$, where now the biggest change in θ_0 occurs for larger h, and the same overall change is spread over a larger range of h.

6 Discussion

The theoretical results derived in this work based on the transformation of the second order linear differential equation to the associated nonlinear first order Riccati equation can only be applied to oceanic observation when using a dimensional depth h (or z). As mentioned above the scale of z equals $\sqrt{(2\tau/\rho)}/f$ so for $\tau = 0.1Pa$, $\rho = 10^3 Kg/m^3$ and $f = 10^{-4}s^{-1}$ a non-dimensional $h = 1$ corresponds to a dimensional depth of $100m$. Accordingly, the limiting values of $h = 10^{-2}$ and $h = 10^2$ in Figures 1, 2, and 3 correspond to dimensional depths of $1m$ and $10^4 m$, respectively.

In conclusion it is instructive to compare the change in the deflection angle that occurs in the piecewise constant case (where $K(z) = \mu$ for $z > -h$ and $K(z) = 1$ for $z \le -h$) when the value of μ varies. The discontinuity of $K(z)$ at $z = -h$ does not permit the use of the proposed Riccati equation algorithm as proposed above. However, a straightforward matching analysis similar to that used in *Dritschel et al.* (2020) yields the contour plot of the deflection angle shown in Figure 4. Notably, a smoothed profile of the eddy viscosity in which $K(z)$ varies continuously near $z = -h$ between the values of μ and 1 (i.e. $K(z)$ varies as $\frac{1}{2}(\mu+1)+\frac{1}{2}(\mu-1)\sin(\pi(z+h)/2\epsilon)$ for $-h-\epsilon \le z \le -h+\epsilon$ with $\epsilon \ll 1$) yields indistinguishable results. These results show that, compared to the uniform $K(z)$ associated with $\mu = 1$ in which case $\theta_0 = 45^o$, the deflection angle decreases for $\mu \le 1$ provided h is sufficiently small and increases for $\mu \ge 1$ provided h is sufficiently large. Clearly, a simple averaging of the eddy viscosities in the two layers yields an erroneous value of the deflection angle.

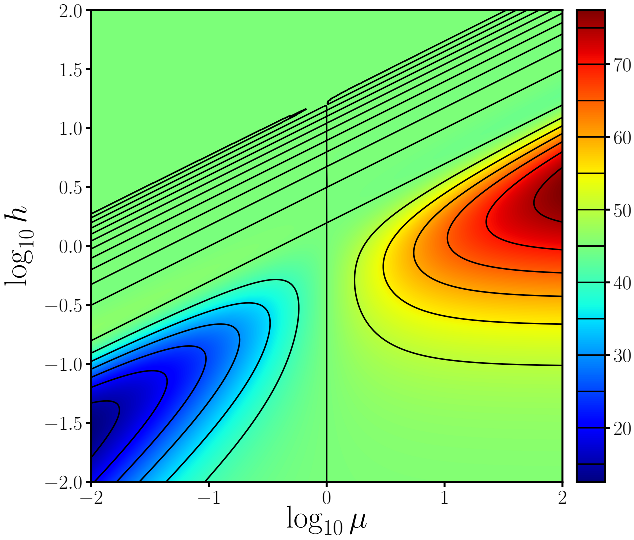

Figure 4: Surface deflection angle θ_0 (in degrees) as a function of the upper-layer eddy viscosity μ and non-dimensional depth h for a piece-wise-constant profile of $K(z)$. Here $K(z) = \mu$ for $z > -h$ and $K(z) = 1$ for $z \leq -h$.

7 Acknowledgments

No data was used in this theoretical paper

References

Bressan, A. and Constantin, A. (2019) The deflection angle of surface ocean currents from the wind direction. *J. Geophys. Res.: Oceans* 124, 7412–7420.

Cariñena, J. F., and Ramos, A. (1999). Integrability of the Riccati equation from a group theoretical viewpoint. *Int. J. Mod. Phys. A* 14, 395–414.

Constantin, A., Frictional effects in wind-driven ocean currents. *Geophys. Astrophys. Fluid Dyn.* (in print), doi.org/10.1080/03091929.2020.1748614

Dritschel, D. G., Paldor, N., and Constantin, A. (2020). The Ekman spiral for piecewise-uniform viscosity. *(submitted)*

Ekman, V. W. (1905). On the influence of the Earth's rotation on ocean-currents. *Ark. Mat. Astron. Fys.* 2, 1–52.

Hille, E. (1997). *Ordinary differential equations in the complex domain.* Dover Publ., New York.

Holmes, M. H. (2013). *Introduction to perturbation methods.* Springer, New York.

Madsen, O. S. (1977). A realistic model of the wind-induced Ekman boundary layer. *J. Phys. Oceanogr.* 7, 248–255.

Polyanin, A. D., and Zaitsev, V. F. (2000). *Handbook of exact solutions for ordinary differential equations.* CRC Press, Boca Raton, Florida.

Röhrs, J., and Christensen, K. H. (2015). Drift in the uppermost part of the ocean. *Geophys. Res. Lett.* 42, 10349–10356.

Schuh, D. (2014). Nonlinear Riccati equations as a unifying link between linear quantum mechanics and other fields of physics. *J. Phys.* 504, 012005.

Wenegrat, J. O., and McPhaden, M. J. (2016). Wind, waves, and fronts: frictional effects in a generalized Ekman model. *J. Phys. Oceanogr.* 46, 371–394.